The Impact of Mediterranean SSTs on the Sahelian Rainfall Season

DAVID P. ROWELL

Met Office, Hadley Centre for Climate Prediction and Research, Bracknell, Berkshire, United Kingdom

(Manuscript received 18 September 2001, in final form 7 August 2002)

ABSTRACT

A variety of regional and global sea surface temperature (SST) patterns are known to affect interannual to decadal variations of summer rainfall over the Sahel, and for most of these patterns considerable progress has been made towards understanding their influence. However, a possible link between Mediterranean SSTs and Sahelian rainfall has yet to be studied, and so the aim of this paper is to use observational and atmospheric general circulation model (AGCM) data to confirm and understand this relationship.

In years when the Mediterranean is warmer than average, it is shown that the Sahel tends to be wetter than normal, whereas in cool Mediterranean years it tends to be drier. The observed data also demonstrate that during the last five decades (1947–96) the strength of this impact has been roughly equal to that of Pacific SSTs, and a little less than that of the tropical Atlantic. Moreover it is most apparent on timescales of a decade or more, although it does also exert some influence at shorter timescales. It is also speculated that the Mediterranean may partly explain the impact of an interhemispheric pattern of SST anomalies found in earlier studies.

Analysis of the AGCM data provides the most convincing evidence that the observed relationship is indeed due to an influence of the Mediterranean on the Sahel. In particular, a pair of idealized experiments forced by warmer (colder) than average SSTs in the Mediterranean, and climatological SSTs elsewhere, produce a clear and significant summer rainfall response over the Sahel. Data from these experiments are then used to explain this impact. If SSTs in the Mediterranean are warmer than average, then local evaporation is enhanced, and the moisture content of the lower troposphere increases. This additional moisture is advected southward across the eastern Sahara by the mean flow, leading to enhanced low-level moisture convergence over the Sahel, which feeds enhanced rainfall. This is then amplified by four positive feedback mechanisms: a more rapid influx of moisture from the tropical Atlantic triggered by enhanced convective heating, a reduced outflow of moisture from the midlevel African easterly jet, an enhanced hydrological cycle, and a larger rainfall contribution from African easterly waves.

1. Introduction

It is well known that interannual and decadal fluctuations of seasonal rainfall over the semiarid Sahel are largely affected by variations of global and regional sea surface temperature (SST) patterns. It has also been suggested that these may be amplified by land surface feedbacks, although the magnitude and mechanistic timescales involved (from days to decades) remain a topic of some debate. The underlying SST variations include anomalies in the tropical Atlantic (e.g., Lamb 1978; Hastenrath 1990; Vizy and Cook 2001); the central and east Pacific (e.g., Folland et al. 1991; Janicot et al. 1996; Rowell 2001, hereafter R01); the Indian Ocean (e.g., Palmer 1986; Shinoda and Kawamura 1994), particularly its gradient to the west Pacific (R01); the Mediterranean (Ward 1994; Rowell et al. 1995; R01); and an interhemispheric contrast of SST anomalies (e.g., Folland et al. 1986, 1991; Rowell et al. 1995) that may include some of the foregoing regional anomalies. For many of these SST patterns, the cited studies, and many others, have proposed plausible mechanisms by which they may affect seasonal rainfall over the Sahel. However, for the Mediterranean link and the interhemispheric link, such detailed analyses have yet to be performed.

The purpose of this paper is to examine the association between Mediterranean SSTs and Sahelian rainfall. Two key issues, among others, are addressed. One is whether their observed correlation actually represents an influence of the Mediterranean on the Sahel, rather than merely some external influence on both regions, or even a Sahelian impact on Mediterranean climate. Since this Mediterranean impact will in fact be confirmed, a second issue then is to determine the mechanism for this regional teleconnection. These are important questions for a region that is highly sensitive to the vagaries of the climate system; for example, the answers should increase our understanding of seasonal prediction for the Sahel and also feed into studies of future climate change over the region.

The paper is arranged as follows. In section 2 ob-

Corresponding author address: Dr. David P. Rowell, Met Office, Hadley Center for Climate Prediction and Research, London Road, Bracknell, Berkshire RG12 2SY, United Kingdom.
E-mail: Dave.Rowell@metoffice.com

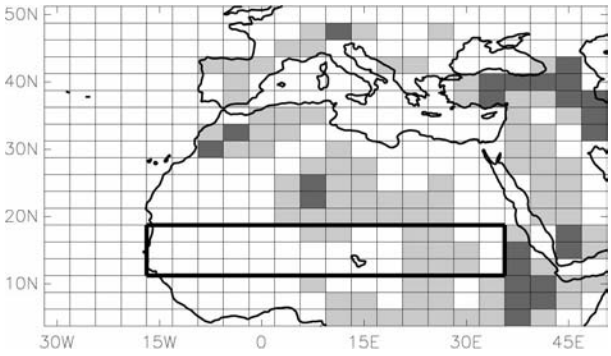

FIG. 1. Location of the Sahel (thick lines), and boundaries of the grid boxes used by the AGCM, precipitation, and SST datasets (thin lines). Shading shows model orography in excess of 500 (light gray) and 1000 m (dark gray).

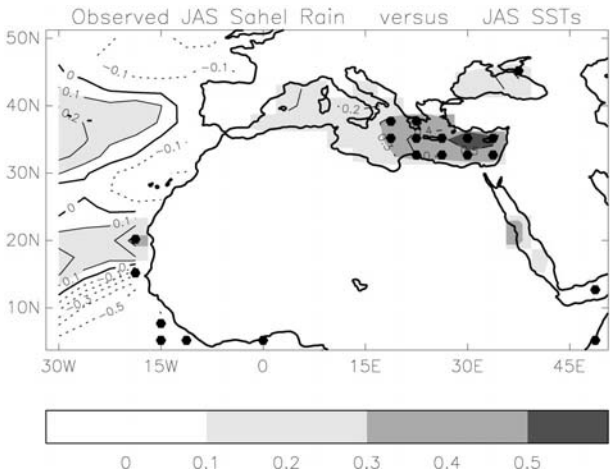

FIG. 2. Correlations between observed Sahel rainfall and SSTs, using Jul–Sep mean data for 1947–96. Contours, at intervals of 0.1, use thin solid lines for positive values, dashed lines for negative values, and a thick solid line for zero. The local rejection of a null hypothesis of zero correlation (at the 5% significance level with a two-tailed test) is indicated by a solid hexagon.

servational data is used to examine the Mediterranean–Sahel relationship in more detail as well as its potential for improving seasonal predictability of Sahelian rainfall. In section 3, data from a variety of integrations with an atmospheric general circulation model (AGCM) are used to provide evidence that the relationship is indeed due a Mediterranean forcing of Sahelian climate. Next, in section 4, the model data are used to examine the mechanism for this relationship, and last, section 5 presents a summary and conclusions.

2. Observed Mediterranean–Sahel relationships

a. Data

The observed rainfall data used in this study derive from two sources. The primary one, used as far as 1996, is an updated version of that described by Hulme (1994), and utilizes monthly mean rain gauge records gridded to a resolution of 2.5° latitude by 3.75° longitude. This is identical to the grid of the AGCM employed in later sections, and is illustrated in Fig. 1. A secondary dataset is that of the Global Precipitation Climatology Project (GPCP) (version 2, Huffman et al. 1997; Susskind et al. 1997), which combines gauge measurements with satellite estimates of rainfall. It is available in near real time on a 2.5° grid, and has been scaled so as to have the same mean and standard deviation as the Hulme data during their overlapping period (1979–96). This is used only for illustrative purposes, to extend the estimates of Sahel rainfall plotted in Fig. 3 (to be shown later) to the most recent years available, 1997–2001. It is not used in any other calculations presented below.

The main period chosen for analysis is the 50-yr epoch 1947 to 1996, which is roughly the longest period over which the quality of rainfall and SST data is close to its peak. Analysis also focuses on July–August–September (JAS) seasonal means, which Rowell et al. (1995), and others, show to be the months of highest rainfall over the Sahel, and Ward (1994) shows to be months of broadly similar relationship to SSTs. Since rainfall estimates are not always available in some grid boxes, it is stipulated that data must be present in all 3 months in order to form a seasonal mean. The area defined as the Sahel is identical to that of R01, encompassing 11.25°–18.75°N, 16.875°W–35.625°E, and is shown in Fig. 1. Time series of Sahelian rainfall were created for both observed and model data by averaging over all available grid boxes for each JAS season.

To verify that the results below are insensitive to the source of rainfall data chosen for 1947–96, a further time series of JAS Sahel rainfall was obtained from S. Nicholson and D. Klotter (2002, personal communication). This was formed from rain gauge records averaged over regions 13 to 20 of Nicholson et al. (2000). Its correlation with the Hulme-based index is 0.99 for 1947–96 and 0.97 for 1983–96 (the two datasets are largely independent for the latter period, whereas prior to 1983 the Hulme data includes many African gauge records from the Nicholson data). Thus, it seems that the analysis presented here will be almost independent of the gauge network and data processing technique employed by the chosen rainfall dataset.

Finally, the SST data derive from the Met Office's latest reconstruction of monthly mean SSTs, known as HadISST1.1 (Rayner et al. 2003). All calculations use JAS means of an interpolated version of the dataset in which the original 1° resolution was degraded to the 2.5° by 3.75° grid used by the model.

b. The SST–rainfall relationship

As noted in the introduction, the association between Sahelian climate variability and a number of SST patterns around the globe is well known. Thus in Fig. 2 attention is focused on correlations between JAS Sahel

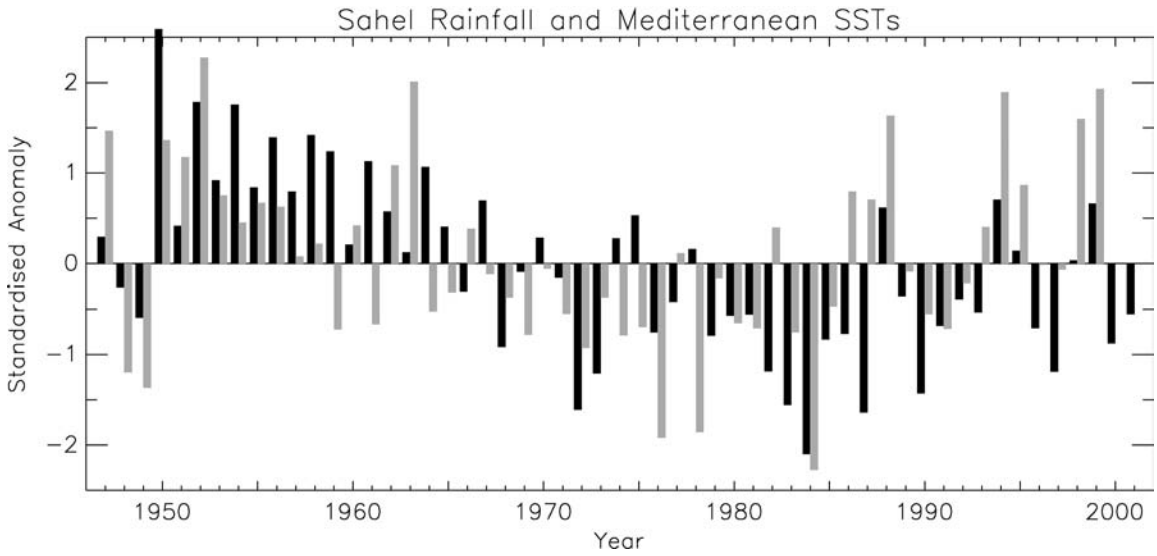

FIG. 3. Time series of rainfall averaged over the Sahel for 1947–2001 (black bars) and the Mediterranean SST index defined in section 2b for 1947–99 (gray bars). All data are Jul–Sep means, and are standardized with respect to 1947–96. Rainfall data are from the Hulme dataset for 1947–96 and the GPCP dataset for 1997–2001.

rainfall and JAS SSTs in the Mediterranean region; local significance is assessed following von Storch and Zwiers (1999), for example, and taking account of serial correlation (Folland et al. 1991). Positive values appear throughout the Mediterranean, and in the east achieve local significance, peaking at $r = 0.57$. Thus a warming of the Mediterranean is often (but not always) associated with enhanced Sahel rainfall.

In order to examine this relationship in more detail, we define an index of those aspects of the Mediterranean that seem most important from a Sahelian point of view. This is achieved by simply averaging each year's JAS SST data over the Mediterranean grid boxes shown to be significant in Fig. 2.

First, we assess the strength of the Mediterranean–Sahel relationship relative to that of other SST–Sahel relationships. This is determined from the correlation between the Mediterranean SST index and JAS Sahel rainfall, which is found to be 0.47 during 1947–96 (significant at the 1% level). Thus this Mediterranean influence on the Sahel is of a similar magnitude to that of the east Pacific or of the west Pacific/Indian Ocean SST gradient, and a little less than that of the tropical Atlantic (R01).

In terms of the timescales of Sahelian rainfall that are affected, the Mediterranean appears to be comparatively more important at explaining part of the recent decadal variability. This is shown qualitatively by Fig. 3, where it seen that during the wet Sahelian decade of the 1950s most years are warmer than average in the Mediterranean, whereas during the drought of the 1970s and 1980s most years have below-average SSTs. Furthermore, this can be quantified by correlating filtered Sahelian and Mediterranean indices: at timescales greater than 8 yr $r = 0.62$ (during 1947–96), whereas at timescales less than 8 yr $r = 0.31$ (a second-order recursive Chebychev filter with 50% amplitude cutoff at 8 yr was used). Assuming these correlations arise because the Mediterranean forces changes over the Sahel, this spectral dependence can be explained by the nature of the Mediterranean SST variability itself, which contains 41% of its variance on timescales more than 8 yr, compared to about 23% expected from a white noise process, resulting in a larger signal-to-noise ratio at decadal timescales.

Next, following the methodology of R01, it can be shown that there have been no significant nonstationarities in the Mediterranean–Sahel correlation throughout the twentieth century (1900–96), based on a 30-yr moving window. In other words, multidecadal variations in the strength of this relationship have been no greater than those expected from the effects of ''weather noise'' or from the effects of random variations in the competing influence of other SST patterns.

Finally, it is important to know whether this relationship is independent of other SST–Sahel relationships, and so correlations between the Mediterranean index and the other regional and global SST patterns known to affect the Sahel have been computed. For the three indices defined by R01, representing the tropical Atlantic, the east Pacific, and the west Pacific/Indian Ocean SST gradient, these each had negligible correlation with the Mediterranean index during JAS 1947–96 ($r = -0.02$ to 0.08). Thus it seems the Mediterranean provides an association with the Sahel that is additional to, and statistically independent of, these other regional SST patterns. However, the correlation between the JAS Mediterranean index and the JAS interhemispheric thermal contrast (ITC) pattern (defined here by the third covariance eigenvector of 1901–80 global SSTs, from

Colman et al. 1997) is slightly stronger at 0.29. At decadal timescales, using low-pass filtered time series, this rises to 0.54. Although neither correlation is statistically significant (at the 5% level, accounting for serial correlation), this nevertheless suggests the possibility that part of the relationship between the ITC and the Sahel may be due to the relationship between the Mediterranean and the Sahel.

c. *Predictability of Sahel rainfall using Mediterranean SSTs*

Given that the Mediterranean appears to affect Sahelian climate variability to roughly the same extent as the more established predictors, and that its impact is largely statistically independent of these predictors, it may itself be an additional candidate predictor of Sahel rainfall. (Note again our assumption that the underlying cause of the Mediterranean–Sahel link is an influence of the former on the latter; this is addressed in section 4.)

If Mediterranean SSTs are to have genuine utility within a predictive system, they must, however, have a lead relationship over JAS Sahel rainfall, as well as a simultaneous relationship. At the Met Office two experimental seasonal forecasts are issued for the Sahel each year, one based on March to April SSTs, and the other on May to June SSTs (Ward et al. 1993; Colman et al. 1997). Hence, Fig. 4 illustrates the relationship between JAS Sahel rainfall and SSTs averaged over each of these two lead seasons. Not surprisingly, correlations are rather less than those of the simultaneous analysis (Fig. 2), although statistical significance is achieved in parts of the western Mediterranean at both leads. This falloff in preseason potential skill is, however, larger than for other ocean basins affecting the Sahel, and is due to weaker persistence of Mediterranean SST anomalies from spring to summer. This is typical of the subtropics, compared to the Tropics, and may reflect a larger influence of chaotic atmospheric dynamics on a shallow mixed layer. Further research is now required to assess the precise extent to which inclusion of a Mediterranean predictor into empirical seasonal forecasts of Sahel rainfall could enhance their skill.

The aim of this paper now is twofold. First, it is to clarify that the correlation between the Mediterranean and the Sahel is indeed due to an impact of the former on the later. Second, it is to understand the mechanisms by which the Mediterranean may have contributed to past climate anomalies over the Sahel, and thus how it may also contribute to future climate anomalies. Both these aims are achieved through the analysis of AGCM data.

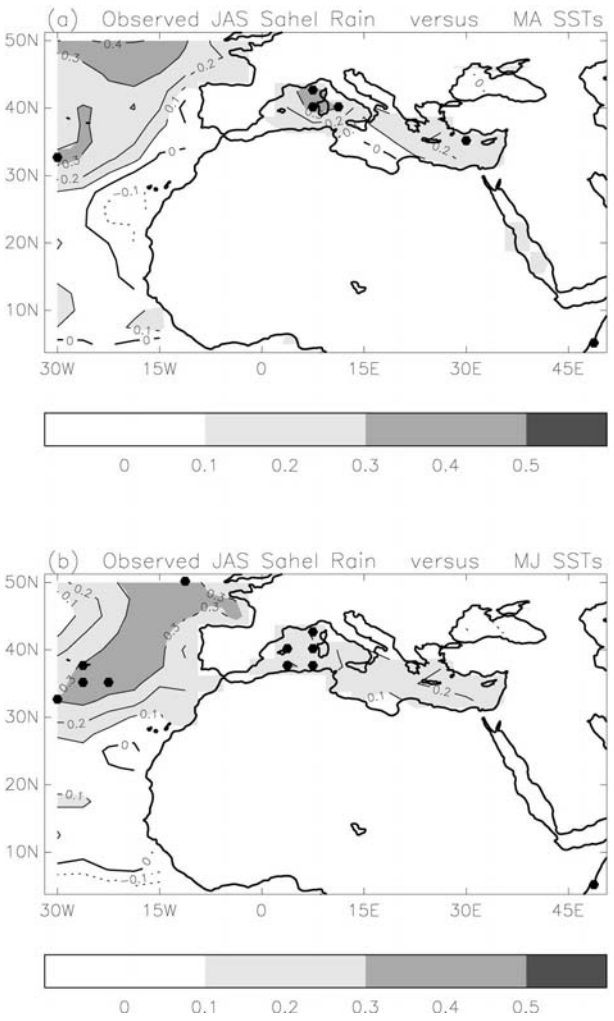

FIG. 4. Correlations between observed Jul–Sep Sahel rainfall and (a) Mar–Apr SSTs, and (b) May–Jun SSTs, both using data for 1947–96. Shading, contours, and identification of local significance are as in Fig. 2.

3. Simulated Mediterranean–Sahel relationships

The AGCM used in this study is the HadAM3 version of the Met Office climate model. It has a horizontal resolution of 2.5° latitude by 3.75° longitude, 19 levels in the vertical, and an atmospheric and land surface physics package outlined by Pope et al. (2000) and references therein.

The model's JAS rainfall climatology over North Africa is illustrated in Fig. 5, which shows this to be moderately well simulated, though a little too wet over the Sahel, and a little too dry further south. Averaging over the Sahelian box of Fig. 1, the model climatology is 3.9 mm day^{-1}, slightly higher than the observed climatology of 3.5 mm day^{-1}.

Two types of simulation data are described here, which are used first to support the observational analysis of a link between Mediterranean SSTs and Sahelian rainfall variability, and second to understand the mechanisms for this regional teleconnection. All model data are treated in the same way as the observational data; see section 2a.

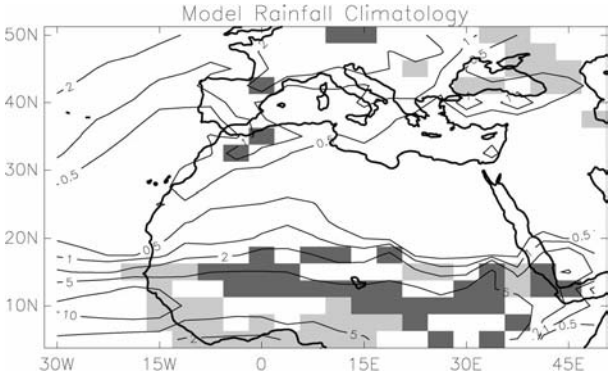

FIG. 5. Simulated Jul–Sep rainfall climatology, using ensemble mean data for 1961–90. Units are mm day^{-1}. Dark gray shows where values exceed the equivalent observed climatology by more than 1 mm day^{-1}, and light gray shows where it underestimates the observed climatology by more than 1 mm day^{-1}.

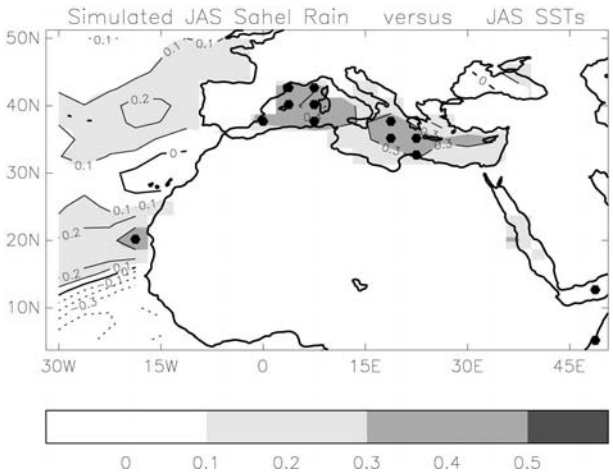

FIG. 6. As in Fig. 2 except using simulated ensemble mean Sahel rainfall.

a. Global SST experiments

The first set of experiments consists of an ensemble of integrations forced primarily by the observed history of global SSTs and sea-ice extents, which aim to simulate past climate variations with maximal skill. Six integrations were carried out, each for the period 1 February 1870 to 30 December 1999. All were forced by the HadISST1.1 data (processed to preserve monthly means; Taylor et al. 2000), and also by variations in total solar irradiance (Lean et al. 1995), and by a representation of the impact of volcanic stratospheric aerosols on optical depth (Sato et al. 1993). The ensemble members differ only in their initial atmospheric conditions, which were taken from an earlier HadAM3 simulation.

The link between the simulated ensemble mean time series of Sahel rainfall and Mediterranean SSTs during 1947–96 is shown in Fig. 6. This is broadly similar to the observed pattern of Fig. 2, showing a tendency for warmer than average SSTs throughout the Mediterranean to be associated with enhanced rainfall over the Sahel. Although the highest values now appear in the western (rather than eastern) Mediterranean, local differences of the correlations between Figs. 2 and 6 are not statistically significant, and are thus within the variability expected from random sampling.

Therefore, given the model's ability to reproduce the observed rainfall–SST correlations when forced only by observed SSTs, we can now discard the conceivable explanation that this relationship might be due to an impact of Sahelian rainfall on Mediterranean climate (rather than vice versa). Thus, of the three possible explanations for the Mediterranean–Sahel link raised in the introduction, two remain: one is that some external SST feature may affect both regions, and the second is that Mediterranean SSTs may indeed affect Sahelian rainfall variability. The following section addresses these possibilities.

b. Idealized SST experiments

The second type of experimental data consists of a pair of integrations forced by idealized SST patterns restricted to the Mediterranean basin, with forcings from all other ocean basins being absent. This provides an effective tool to address two critical issues. First, it will enable us to understand whether the Mediterranean–Sahel correlation is indeed due to an influence of the Mediterranean on the Sahel, rather than merely due to a statistical link arising from a third-party influence on both regions. Second, these experiments will provide a ''clean'' source of data with which to identify the mechanism for this regional teleconnection, without the confounding influence of circulation changes arising from other forcings.

The experiments are forced by the anomalous SSTs shown in Fig. 7, which depict opposite signs of a single pattern, whereby one experiment broadly represents a warming of the Mediterranean, and the other a cooling. This pattern is designed to be of maximal relevance to the Sahel, and so is directly proportional to a map of the regression coefficients of observed JAS Sahel rainfall onto JAS SSTs in the Mediterranean. The amplitude of this pattern is then made to vary throughout the annual cycle, such that its size in each month equates to two interannual standard deviations of anomalous SST. (This was achieved by projecting the preceding regression pattern onto monthly mean SSTs for 1961–90, then computing the interannual standard deviation of this time series for each calendar month, next smoothing this 12-point annual cycle with a 1-2-1 filter, and finally multiplying the regression pattern by double these standard deviations to obtain an annual cycle of forcings in units of SST.) This produces a forcing that has strong but realistic amplitude, and plausible seasonality. These 12 monthly anomaly patterns were then added to (or subtracted from) a seasonally evolving 1961–90 SST climatology, and this single year repeated 20 times. Thus

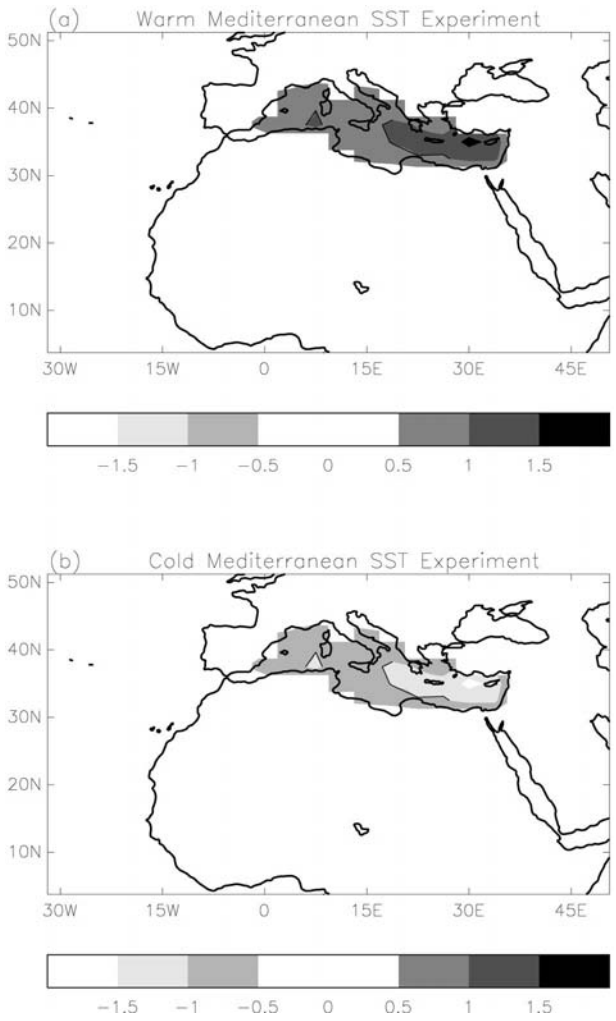

FIG. 7. Forcing patterns used in the idealized SST experiments: (a) warm Mediterranean expt, and (b) cold Mediterranean expt. Averages from Jul–Sep are shown, and units are °C.

two continuous 20-yr integrations were carried out with anomalous forcing in the Mediterranean and climatological SSTs elsewhere, in effect creating a pair of 20-member ensembles.

Figure 8 shows the regional impact of these Mediterranean SST anomalies on rainfall, using a composite difference analysis along with a *t* test to assess local significance. A small, but not surprisingly significant, impact is seen over the Mediterranean, with the warmer SSTs producing more rainfall over the west and central Mediterranean, but drier conditions at its easternmost part. To the south, the diminutive climatological rainfall over the arid Sahara is significantly enhanced, and crucially for this study, the wet season over the Sahel is significantly more abundant. Averaged over the Sahel as a whole, JAS mean rainfall is 1.2 interannual standard deviations higher in the warm Mediterranean experiment than in the cold experiment.

Thus, this provides further and convincing evidence

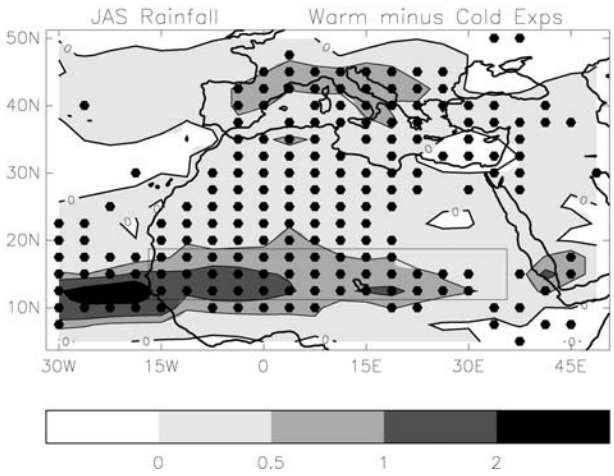

FIG. 8. Composite difference of Jul–Sep rainfall, computed as the average of 20 warm-expt years minus 20 cold-expt years. Units are mm day^{-1}, and the local rejection of a null hypothesis of zero difference (at the 5% significance level with a two-tailed test) is indicated by a solid hexagon. Sahel location is marked by rectangular box.

that SST variability in the Mediterranean does indeed affect seasonal rainfall totals over the Sahel. Furthermore, this analysis and that of section 3a suggest that the model can now be used to deduce a mechanism for this link.

4. A mechanism linking the Mediterranean to the Sahel

a. Seasonal mean analysis

The approach taken here to understand the mechanism for this regional teleconnection is to first determine the source of the additional moisture required to feed the enhanced rainfall over the Sahel in warm Mediterranean years. There are two possibilities: one is increased evaporation, and the other is additional moisture convergence in the atmosphere above the Sahel. Presumably both may play a role, and must then be triggered or maintained externally (this will form the next step of the investigation; to be discussed later).

Figure 9 shows the impact of Mediterranean SSTs on the model's surface evaporation using data from the idealized SST experiments. Not surprisingly the largest impact is over the Mediterranean itself, where a considerable increase is seen when SSTs are warmer than average. A smaller (but statistically significant) increase in evaporation is apparent over much of the Sahel, and also an even smaller rise over the Sahara. Farther south, evaporation is actually reduced, which is because of larger increases in cloud cover, leading to reduced surface heating (not shown). Over the Sahel, rainfall events are sufficiently frequent (almost daily in the model, and every 2–3 days in reality; Le Barbé et al. 2002) that some of the additional moisture evaporating from the wetter surface remains within the Sahelian atmosphere

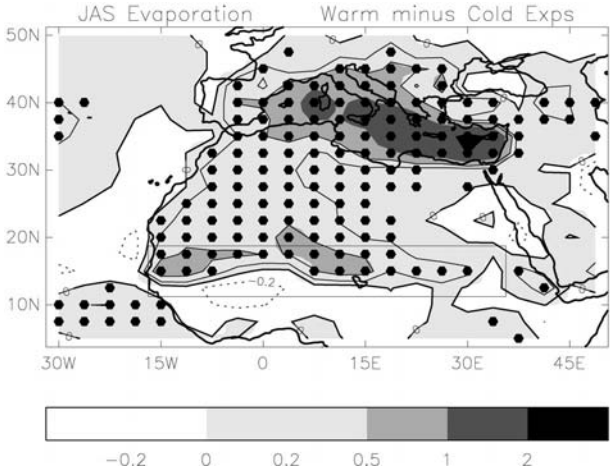

FIG. 9. Composite difference of Jul–Sep evaporation, computed as the average of 20 warm expt years minus 20 cold expt years. Units are mm day^{-1}, contours are plotted as shown on bar, and the local rejection of a null hypothesis of zero difference (at the 5% significance level with a two-tailed test) is indicated by a solid hexagon.

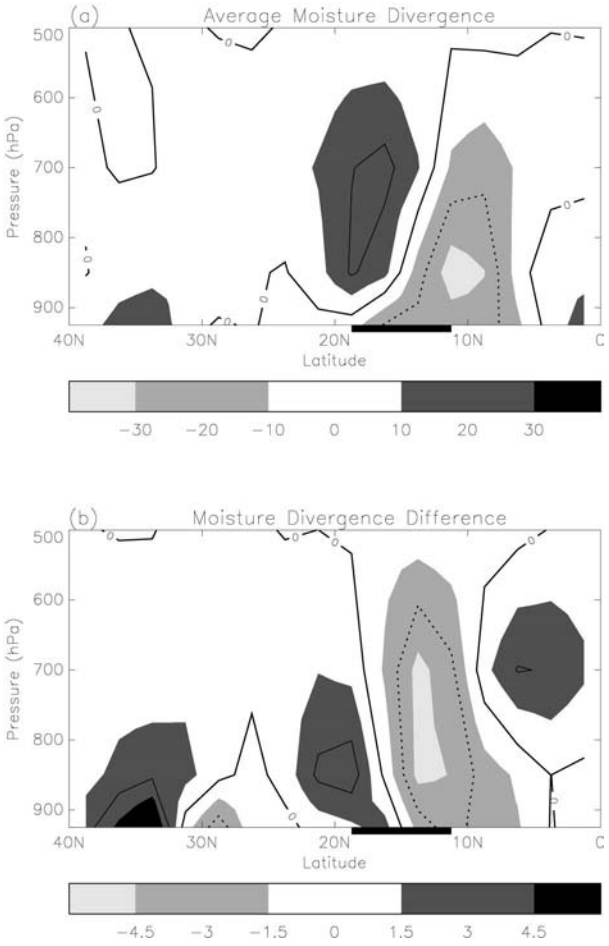

FIG. 10. (a) Cross section of average moisture divergence, computed over all 20 yr of both warm and cold expts. (b) Cross section of the composite difference of moisture divergence, computed as the average of 20 warm-expt years minus 20 cold-expt years. In both (a) and (b), data are Jul–Sep means averaged over 15°W–37.5°E, units are g kg^{-1} s^{-1}, contours are plotted as shown on bar, and Sahel location is marked by a solid rectangle beneath the *x* axis.

before being returned to the ground by a further rainfall event. However, a significant proportion must also be advected out of the Sahel, that is, that which is evaporated too long before the next rainfall event or has experienced mainly meridional advection. Thus, the component remaining within the Sahelian atmosphere becomes available to help feed subsequent rainfall here, and the whole process can be viewed as a small enhancement of the regional hydrological cycle, so providing a positive feedback effect on the total Sahelian rainfall increase.

Although changes in evaporation contribute to the additional moisture that feeds greater rainfall over the Sahel, the primary source must be an increase in atmospheric moisture convergence above this region. To study this further, Fig. 10a shows the north–south profile of mean moisture divergence in the lower troposphere over North Africa, using data from the idealized SST experiments at 1200 UTC. First, it is important to explain the relevance of analyzing only midday data. Tropical rainfall exhibits a large diurnal cycle, and this interacts strongly with local atmospheric dynamics; Rowell (1990) illustrates this for the North African region. In order to gain a clear and consistent picture of the circulation changes that induce seasonal rainfall anomalies, the atmospheric data must thus be averaged over only that part of the diurnal cycle when the majority of rain falls. For HadAM3, this is during daylight hours, mainly when the sun is at its highest, and for this the simplest technical solution is to average only those fields produced at 1200 UTC. (Note that in the real world, rainfall extends into the evening and nighttime hours due to the self-sustaining thermodynamics of the squall lines. Like all GCMs, the Met Office model has too coarse a resolution to represent these systems, but since the model's seasonal mean response to SSTs is similar to that observed, we surmise that its error in diurnal phasing does not negate the results of this paper.)

Consider now the pattern of mean moisture divergence shown in Fig. 10a. The intertropical convergence zone (ITCZ) is clearly apparent, centered on 10°N, with the strongest convergence of moisture occurring below about 800 hPa. To the north, is a region of moisture divergence associated with both the African easterly jet (AEJ; see later) and subsidence over the southern Sahara. The composite difference of moisture divergence between warm and cold experiments is shown in Fig. 10b. As anticipated earlier, this shows a substantial increase in moisture convergence over the Sahel when warm SSTs in the Mediterranean are applied. This anomaly is largest from about 850 to 700 hPa, and by comparison with Fig. 10a represents both an intensification of the ITCZ and a northward shift of its northern edge.

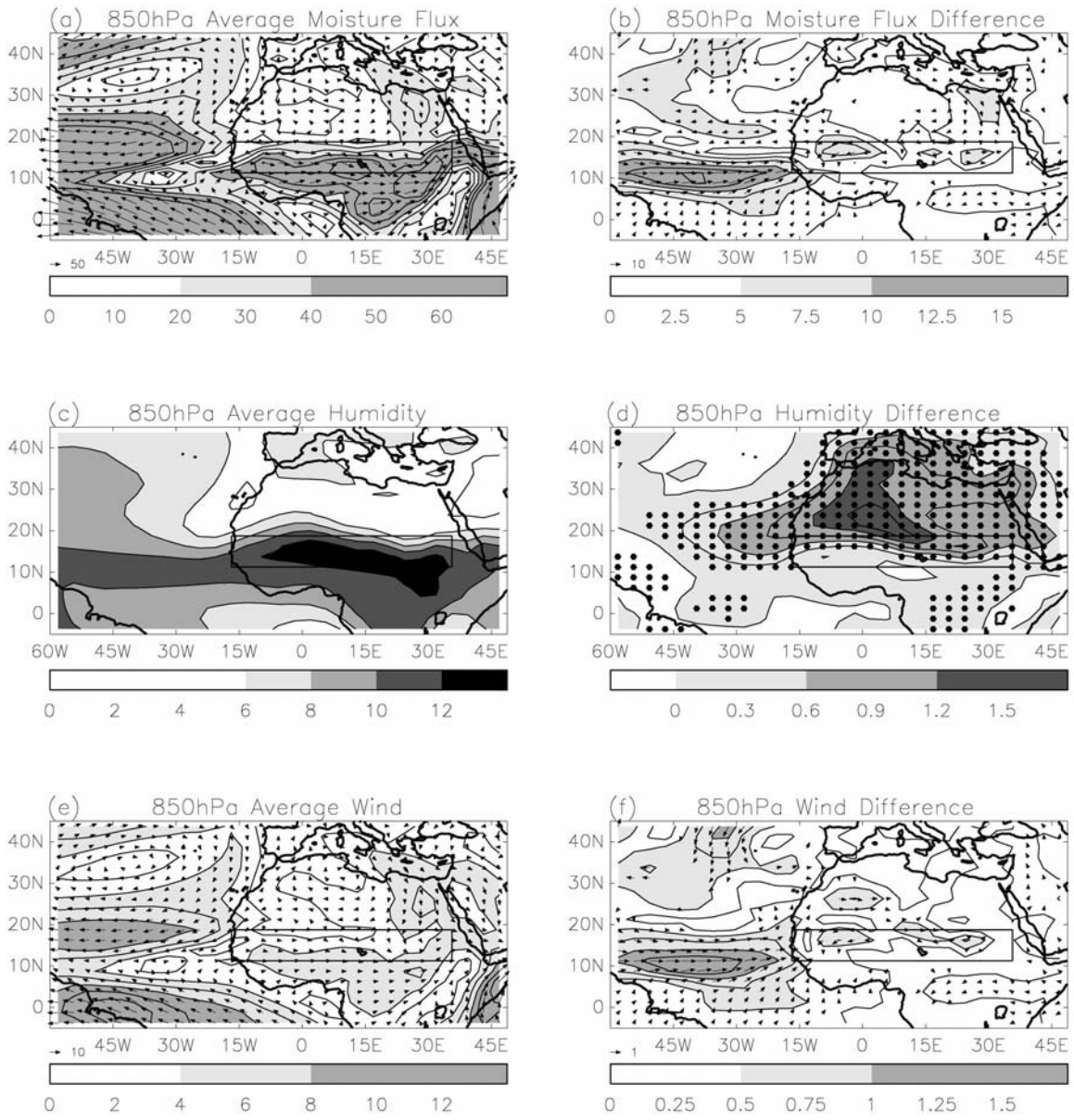

FIG. 11. (a) Average 850-hPa moisture flux (m s^{-1} g kg^{-1}), (b) composite difference of 850-hPa moisture flux (m s^{-1} g kg^{-1}), (c) average 850-hPa specific humidity (g kg^{-1}), (d) composite difference of 850-hPa specific humidity (g kg^{-1}), (e) average 850-hPa winds (m s^{-1}), (f) composite difference of 850-hPa winds (m s^{-1}). All data are Jul–Sep means, averages are computed over all 20 yr of both warm and cold expts and composite differences are computed as the average of 20 warm-expt years minus 20 cold-expt years. Contours are plotted as shown on bar, and for (a),(b), (e),(f) these show the magnitude of the moisture flux or winds. In (b) and (f) vectors are only plotted where the null hypothesis of zero difference between either the u or v components can be rejected (at the 5% significance level with a two-tailed test); and in (d) points where this null hypothesis can be rejected are indicated by a solid hexagon. Sahel location is marked by a rectangular box.

The next issue to address is to ask how the additional moisture is transported into the Sahel in order to maintain this enhanced moisture flux convergence. First we consider the 850-hPa level, noting that similar results are found at 925 hPa (the latter is not shown). Figure 11a shows the mean 850-hPa moisture flux pattern at 1200 UTC. Clearly there are two sources of moisture for the Sahel at this level: the main one is from the tropical Atlantic, via the southern and western coasts of West Africa, and the second, weaker source, is from the Mediterranean, via the eastern Sahara. From Fig. 11b, it is clear that the moisture supply from both these sources is significantly enhanced when the model is forced by warmer than average SSTs in the Mediterranean.

To examine this further, Figs. 11c–f illustrate the mean and response fields for 850-hPa specific humidity

and winds. From these, the following mechanism for the enhancement of Sahelian rainfall may be proposed. Warmer than average SSTs in the Mediterranean lead to enhanced local evaporation (Fig. 9), and hence to enhanced lower-tropospheric humidity here (Fig. 11d). This additional moisture is then advected across the arid eastern Sahara (Fig. 11c) by the mean flow (Fig. 11e), which feeds enhanced moisture convergence over the Sahel, and hence enhanced rainfall. Note that the wind field itself is not significantly altered over the desert (Fig. 11f), but that the anomalous moisture transport (Fig. 11b) arises only through increased moisture availability. However, this probably accounts for only a part of the rainfall increase: a positive feedback mechanism is also proposed, whereby the additional convective heating over the Sahel (Fig. 8) causes more moisture to be drawn in from the tropical Atlantic (Fig. 11b). This supposition of a secondary dynamical response, is supported by Fig. 11, which shows that the enhanced moisture flux from the Atlantic is almost entirely due to a significant change in circulation (Fig. 11f), drawing moisture into the Sahel more rapidly, with the humidity field being relatively unaltered (Fig. 11d).

Now consider the role played by moisture convergence anomalies at 700 hPa (Fig. 10b). The mechanism by which these are maintained is rather different from that at the lower levels, and is examined with the aid of Fig. 12. Figure 12a shows that on average the Sahel receives a weak supply of moisture from the Mediterranean at this level, but experiences a strong export of moisture to the west due to the AEJ. This leads to the net divergence of moisture shown by Fig. 10a. In the idealized experiment with warm SSTs, the influx of moisture from the Mediterranean is enhanced, and the export of moisture by the AEJ is reduced (Fig. 12b). Thus the net export of moisture at this level is reduced, so contributing to the rainfall increase. This can be explained by two distinct mechanisms. First, the enhanced Mediterranean evaporation also leads to higher local humidity at this level, which increases the moisture content of the mean 700-hPa flow across the eastern Sahara (Figs. 12b,d,e). This provides an additional (but weak) moisture source that helps feed enhanced rainfall over the Sahel. The more important mechanism, however, is a positive feedback resulting from the Sahelian rainfall increase. It is well known that in these wetter years over the Sahel the strength of the AEJ is diminished (Newell and Kidson 1984; Fontaine et al. 1995). This probably occurs partly because the north–south gradient of soil wetness becomes weaker, which leads to reduced gradients of evaporation (Fig. 9) and surface temperature, so reducing low-level baroclinicity which is a prime cause of the AEJ (e.g., Hastenrath 1991; Cook 1999), and also because anomalous upward convective transport of low-level westerly momentum weakens the easterlies above (e.g., Kershaw and Gregory 1997). This weakening of the AEJ is clearly seen in the warm SST experiment (Figs. 12e,f), and leads to a fall in the 700-hPa moisture divergence over the Sahel. This then leads to a further increase of Sahelian rainfall. Such a feedback mechanism has also been proposed by Cook (1999), involving the AEJ, midlevel moisture divergence and surface wetness, and by Rowell et al. (1992) but involving the latitude, rather than intensity, of the AEJ.

In conclusion, these idealized experiments have illuminated a number of mechanisms by which the Mediterranean impacts the Sahel, each of which can be seen in the seasonal mean data. First, a ''direct'' mechanism is advection by the mean flow of moister air from the Mediterranean, across the Sahara into the Sahel, primarily at 850 and 925 hPa and more weakly at 700 hPa. Second, this leads to three positive feedback mechanisms in the model, one involving a more rapid influx of moisture from the tropical Atlantic, another involving a weaker export of moisture by the AEJ, and the third involving a greater recycling of moisture through surface evaporation.

b. Subseasonal analysis

In addition to the Mediterranean–Sahel mechanisms already discussed, it is possible that other mechanisms may operate on subseasonal timescales, which could be hidden by the above analysis of seasonal means. The aim of this section is to reveal any such mechanisms.

To examine whether the Mediterranean has any impact on subseasonal rainfall variations over the Sahel, information is required on the amplitude of such variations for a range of timescales and longitudes, in order to facilitate a comparison with the known modes of variability affecting the Sahel (note that the latitude, 15°N, is already specified by the scope of the study). Thus, a helpful way to provide such information is to compute spectra of daily precipitation data from the two idealized SST experiments, and display these as contours of spectral density on a longitude–frequency plot. So, first, for each longitude along the length of the Sahel (and for longitudes 15° beyond the Sahel) rainfall totals for the 3 grid boxes spanning the Sahel (12.5°, 15°, and 17.5°N) were averaged for each day in each of the two Mediterranean experiments. Periodograms were then derived from this daily data, separately for each longitude, for each JAS season, and for each experiment. These were then averaged over the 20 available years, and the resulting longitude–frequency matrices (one for each experiment) smoothed in the frequency domain with a three-point running mean.

Figure 13a shows the estimated climatological rainfall spectrum at each longitude, computed by averaging the periodograms of the two experiments. The first-order impression across the entire Sahel is broadly that of a red noise process. However, in the western Sahel, a spectral peak of around 4 days is superimposed on this variability (seen by the tilting of contours towards high spectral density as periods increase from 4 to 7 days).

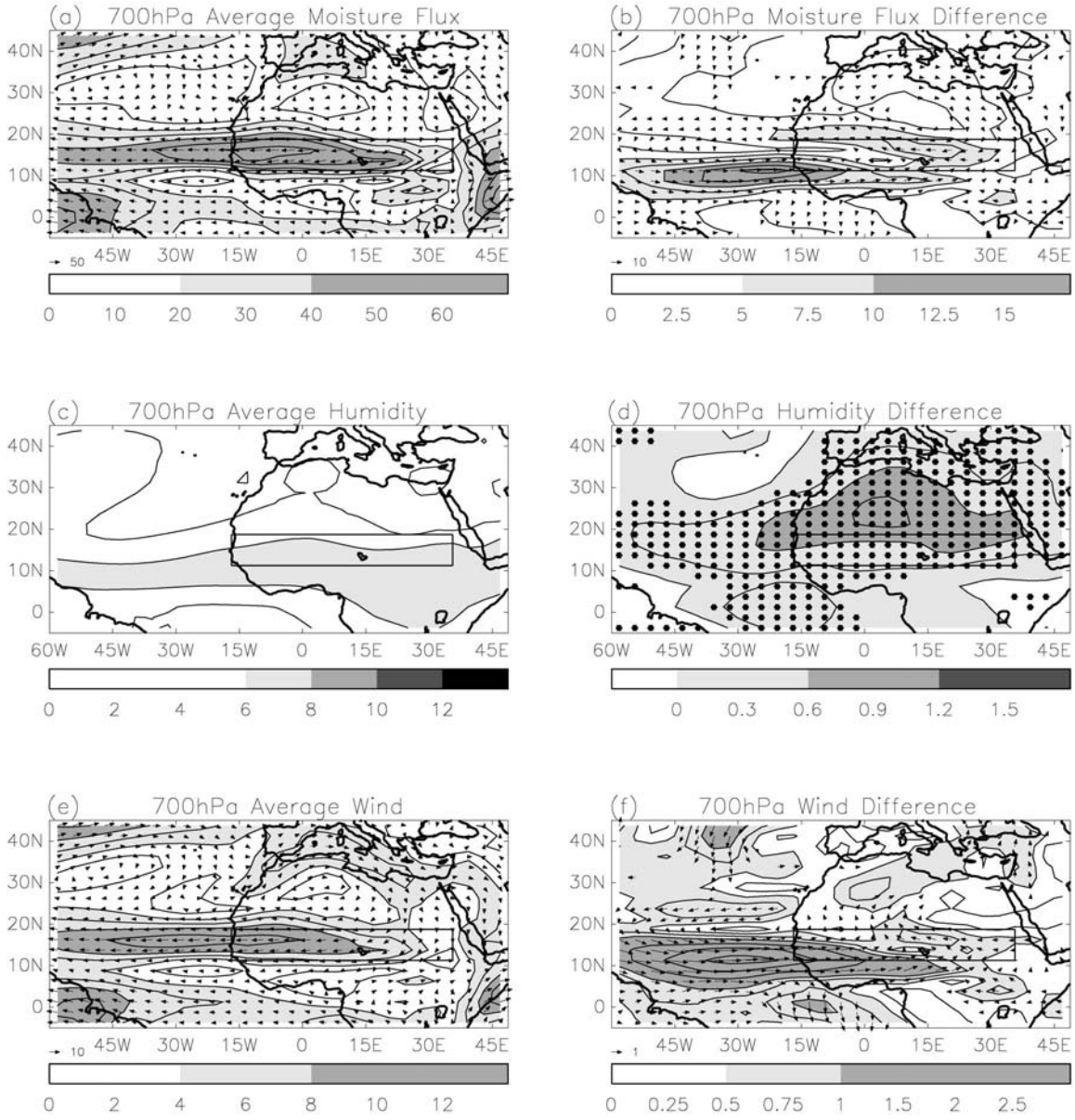

FIG. 12. As in Fig. 11 but at 700 hPa. Note that contour and shading intervals are identical, apart from additional and more widely spaced contours in (f).

This geographic and spectral location matches that expected from African easterly waves (AEWs), which have their strongest amplitude towards the coast of West Africa (e.g., Albignat and Reed 1980; Thorncroft and Rowell 1998) and an observed timescale of about 3 to 5 days (e.g., Burpee 1974; Albignat and Reed 1980).

To demonstrate the impact of the Mediterranean on simulated subseasonal variability, Fig. 13b shows the ratio of spectral densities in warm years to cold years, highlighting points that are significantly different from unity using an F test. Two particular features are apparent. One is that variability increases at all frequencies (and all longitudes), indicating a larger-amplitude red noise process, consistent with increased seasonal rainfall in warm Mediterranean years. The second effect is that this enhancement of variability is much stronger at the timescale and longitude of the AEWs, indicating that they make a proportionally larger contribution to the net rainfall increase than that of other convective events. Thus, although a part of the enhancement of AEW rainfall must be due to the general enhancement at all timescales, it appears that the amplitude or structure of these weather systems also alters in such a way that further amplifies their contribution to rainfall in warm Mediterranean years. This could either be due to dynamic or thermodynamic feedbacks within the AEWs, or due to

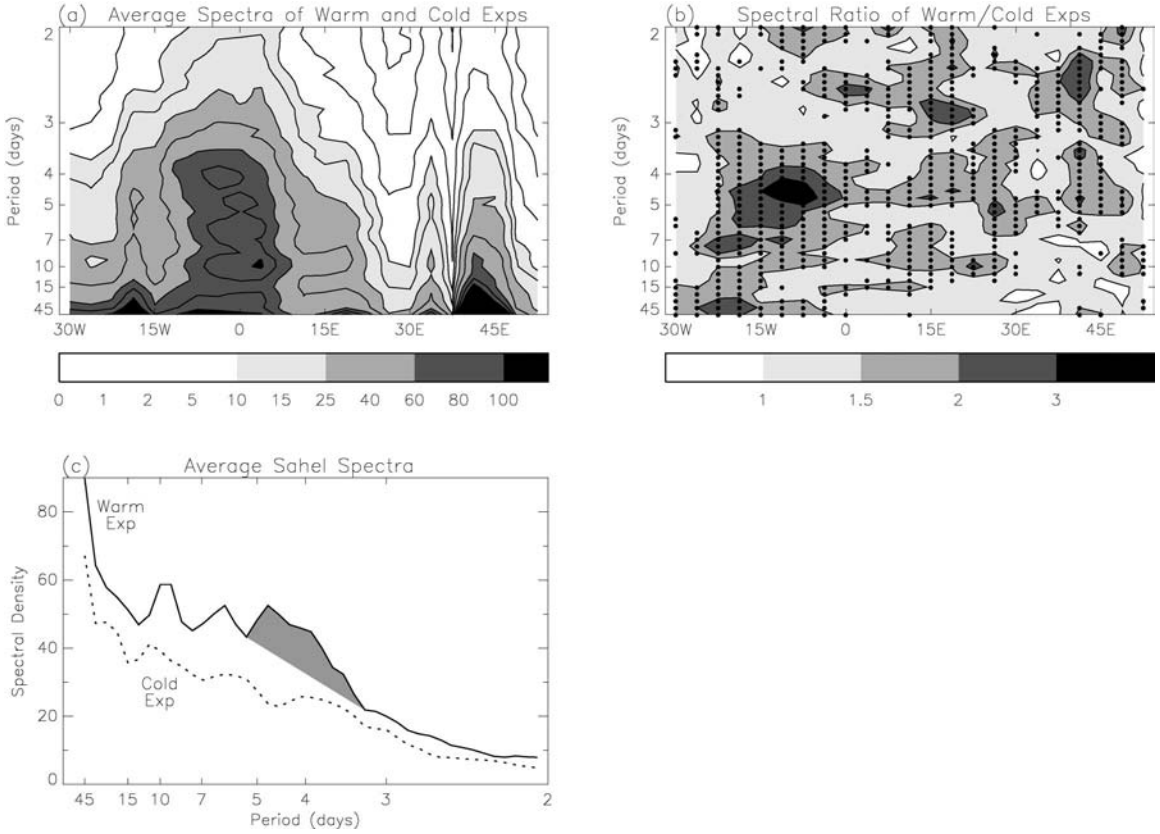

FIG. 13. (a) Longitude–frequency cross section of the average spectral density of daily rainfall for the warm and cold Mediterranean experiments. Data are from Jul–Sep and averaged over 11.25°–18.75°N. Units of spectral density are 10^{-2} mm^2 day^{-2}, and contours are plotted at values shown on bar. (b) Longitude–frequency cross section of the ratio of spectral density of daily rainfall for the warm to cold Mediterranean experiments. The local rejection of a null hypothesis of equal variances (at the 5% significance level with a two-tailed test) is indicated by a solid circle. (c) Averaged spectra of daily Sahel rainfall, from 15°W to 37.5°E, for the warm and cold Mediterranean experiments. Units are 10^{-2} mm^2 day^{-2}, and the shaded area estimates the component of additional rainfall variability in the warm expt due to African easterly waves.

the impact of other atmospheric features to which AEWs are more sensitive. Further work is now required to establish whether this additional AEW-rainfall increase is unique to HadAM3 (requiring similar experiments with other AGCMs and idealized models), and to identify more precisely the mechanisms involved (requiring observed and model-based process studies).

Finally, to estimate the relative importance of this AEW contribution to the seasonal mean response, Fig. 13c compares the average Sahel rainfall spectra between warm and cold Mediterranean experiments. The shaded area represents a rough estimate of the component of additional subseasonal rainfall variability in the warm experiment due to the increase in AEW rainfall (excluding that merely due to the enhanced red noise process). Clearly this represents a small but notable portion of the total change in subseasonal variability (the latter being the total area between the two curves), indicating that this AEW contribution to the model's Sahel rainfall response to Mediterranean SSTs is also small but notable.

c. *Verification issues*

The regional teleconnection mechanisms described in the preceding have been entirely based on an analysis of HadAM3 data. Ideally these should be supported (or refuted) by an analysis of independent datasets. In particular, the proposed mechanisms involve a number of feedbacks, not all of which are necessary to sustain the conclusion of a Mediterranean influence on the Sahel (although the reality of this underlying influence, by whatever mechanism, seems assured from the combination of observed and model evidence). For example, it is possible that one or more of these feedbacks may differ between models, or between HadAM3 and reality, due to the formulation of the convection scheme (and its impact on the large-scale flow), the formulation of the boundary layer scheme (which determines evaporation over ocean and land surfaces), or the model's resolution (which may affect AEW dynamics and orographic influences on the flow).

One potential source of support may lie in the re-

analysis of observational data, particularly that carried out by the National Centers for Environmental Prediction (NCEP) and the National Center for Atmospheric Research (NCAR) (e.g., Kistler et al. 2001), which in theory covers a sufficiently lengthy period to obtain statistically robust results. However, there are a number of complicating factors with this approach: (a) the readily available monthly mean data are averaged over four time points in the diurnal cycle, rather than only 1200 UTC as used here; (b) SST forcing is present in all ocean basins, rather than only in the Mediterranean as above (this would add a further source of noise to a mechanistic analysis, due to the additional influence of non-Mediterranean SST anomalies on the regional circulation); (c) Janicot et al. (2001) recommend that NCEP–NCAR reanalysis data prior to 1968 be discarded for climate variability studies over and around the Sahel due to an apparent impact of unreliable and undersampled observational input (this would further enhance the noise due to sampling error, through the use of only 30 yr of data, compared to 50 yr, or the 2×20 AGCM years above); (d) Janicot et al. (2001) state that even for the 1968–97 period the reanalysis data are not sufficiently accurate for investigating *decadal* variability over this region, and thus recommend restricting analysis to high-pass filtered data (this would further weaken the signal-to-noise ratio, since section 2b showed that the Mediterranean–Sahel relationship is weaker at subdecadal timescales); and (e) other observational network inhomogeneities and model dependencies also exist in the reanalysis data.

To assess the sensitivity of a verification using reanalysis data to these issues, the available HadAM3 data was used within a self-consistent framework to test the impact of items a–d. This was achieved by creating versions of Figs. 10–12 using the following data to address, in turn, items a–d above: (i) data from the idealized SST experiments *averaged over all time steps*; (ii) data from the *experiments forced by global SSTs* averaged over all time steps, and compositing years with the strongest anomalous Mediterranean SST index (17 warm yr and 17 cold yr from 1947–96); (iii) data from the global SST experiments *for 1968–97 only* (compositing 10 warm years and 10 cold years); and (iv) *high-pass filtered data* from the global SST experiments for 1968–97 (using the same 8-yr filter as section 2b, and again compositing 10 warm years and 10 cold years). The combined impact of all these changes, revealed by analysis (iv), was unfortunately such that evidence for many of the mechanisms described in section 4a was overwhelmed by other sources of regional variability. The remaining statistically significant results were a slight increase in humidity at 925–700 hPa over much of North Africa and a slight strengthening of the low-level moisture flux from the Mediterranean into northern Libya and Egypt (not shown). For the moisture divergence analysis (Fig. 10), aliasing of the diurnal cycle (item a) was the critical problem, whereas for the circulation analysis (Figs. 11–12), items b–d had a cumulative negative impact on signal-to-noise levels. Even so, high-pass filtered NCEP–NCAR reanalysis data for 1968–97 were also analyzed, using the same compositing technique. Given the results from global SST experiments, and the particular difficulties associated with moisture-related aspects of the reanalysis data (e.g., Trenberth and Guillemot 1998), it is not surprising, however, that these data were also unable to properly reproduce the regional teleconnection mechanisms of the idealized SST experiments. Finally, it is noted that similar results can be expected if the daily precipitation analysis (Fig. 13) were computed from global simulation or reanalysis data, although this was not undertaken due to the substantial data processing required.

In summary, this section illustrates the difficulties in evaluating the mechanisms of a particular teleconnection whose influence competes with that of other teleconnections, using only a short data record. With reanalysis data, these problems are compounded if the teleconnection is most apparent at decadal timescales. This demonstrates the value of idealized SST experiments, in which the forcing under investigation is isolated from all other forcings. It must be emphasized however that an inability to verify the proposed feedback mechanisms using 30 yr of globally forced high-pass filtered data in no way undermines the importance of this teleconnection. The relative (and notable) contribution of Mediterranean SST anomalies to JAS Sahel rainfall totals was discussed in section 2b. Nevertheless, more work is now needed to corroborate the mechanisms suggested here, in particular an analysis of several long homogeneous time series of midday radiosonde data, and of idealized Mediterranean SST experiments performed with different AGCMs that are also realistic over the North African region.

5. Summary and conclusions

The possibility of a link between the Mediterranean and the Sahel has been investigated here, and a variety of data used to show that anomalies of Mediterranean SSTs have a clear and significant impact on wet season (July to September) rainfall totals over the Sahel. This is such that years with warmer then average SSTs are often wetter over the Sahel, whereas years with cooler than average SSTs tend to be drier. Observational analysis showed that the strength of this impact is as great as that of ENSO, and only a little less than that of the tropical Atlantic. The Mediterranean's influence is strongest on decadal timescales, due to the ''redness'' of its own spectrum (though it does also affect interannual timescales), and may also explain some of the link between an interhemispheric SST pattern and the Sahel. It seems that the Mediterranean may be a part of this pattern, although further experimentation is clearly required to assess the degree to which these global-scale

SST variations affect the Sahel via the Mediterranean and via other ocean regions.

Analysis of AGCM data has been a key aspect of this study. First, it has provided convincing evidence that the observed statistical link between the Mediterranean and the Sahel is indeed due to an influence of the former on the latter. Notably, idealized experiments in which the model was only forced by anomalous SSTs in the Mediterranean (with climatological SSTs elsewhere) produced a strong and significant response in seasonal rainfall over the Sahel. Second, because of the similarity between observed and model responses to the observed history of global SSTs, the AGCM data could be used to understand the mechanism of this regional teleconnection. It was shown that in years when SSTs in the Mediterranean are warmer than average (using the idealized SST experiments), increased evaporation leads to an enhanced moisture content of the air that is advected southwards by the low-level mean flow across the eastern Sahara into the Sahel. This then feeds increased moisture convergence in the lower troposphere over the Sahel, leading to increased rainfall. This initial response is then further enhanced by four positive feedback mechanisms. The first is that the additional convective heating over the Sahel induces a stronger low-level inflow from the tropical Atlantic, which draws moisture in more rapidly, feeding further convection. A second feedback is that enhanced rainfall leads to a weaker midlevel African easterly jet, either via weaker surface temperature gradients southwards from the Sahel, or via enhanced convective transport of low-level momentum. This reduces the 700-hPa export of moisture from the Sahel, again leading to enhanced moisture availability to feed a further rainfall increase. Another feedback operates simply through an enhancement of the hydrological cycle, whereby increased evaporation over the Sahel feeds increased rainfall. The final mechanism is that the component of rainfall due to African easterly waves is enhanced to a greater extent than that due to other convective activity. Each of these responses tends to be reversed in years when the Mediterranean is cooler than average. Further work is now required to investigate whether all these mechanisms occur in reality and in other AGCMs, and to understand their action in greater detail.

Finally, the results of this paper are also relevant to the predictability of Sahel rainfall. On seasonal timescales, the persistence of Mediterranean SST anomalies is weaker than that of other SSTs affecting the Sahel, but even so their preseason correlation with the Sahel remains statistically significant in some parts of the Mediterranean. One issue for further study is the extent to which they are already included in empirical seasonal forecasts by using the interhemispheric SST pattern; this requires a detailed assessment using longer data periods, independent training, and model experimentation. Another important issue is whether additional predictive skill could be obtained by understanding the preseason evolution of the Mediterranean SST anomalies themselves. In particular, it would be useful to determine whether their more rapid evolution is mainly due to chaotic atmospheric dynamics, or whether it is also partly due to teleconnections that could perhaps be predicted. On multidecadal timescales, ''global warming'' is likely to be the dominant factor, and here a warmer Mediterranean may contribute additional moisture to the Sahelian wet season. However, it remains to be seen whether the net impact (i.e., including that of other SST regions) will be a more or less abundant rainy season over the Sahel.

Acknowledgments. I am very grateful to Ian Macadam who ran the model experiments, with assistance from David Sexton. This study was supported by the UK Public Meteorological Service Research and Development Programme (Contract MSG-2/00), and the EU ''PROMISE'' Project (Contract EVK2-CT-1999-00022). Rainfall data were kindly supplied by Mike Hulme (with support from the UK DETR, Contract EPG-1/1/85) and by Sharon Nicholson, and the ITC SST time series was provided by Andrew Colman. I have also benefited from comments on an earlier version of the manuscript by Serge Janicot, Chris Thorncroft, and Richard Jones.

REFERENCES

Albignat, J. P., and R. J. Reed, 1980: The origin of African wave disturbances during Phase III of GATE. *Mon. Wea. Rev.,* **108,** 1827–1839.

Burpee, R. W., 1974: Characteristics of North African easterly waves during the summers of 1968 and 1969. *J. Atmos. Sci.,* **31,** 1556–1570.

Colman, A. W., M. D. Davey, M. Harrison, A. Evans, and R. Evans, 1997: Multiple regression and discriminant analysis predictions of Jul–Aug–Sep 1997 rainfall in the Sahel and other tropical North African regions. *Experimental Long-Lead Bulletin,* Vol. 6, No. 2, 33–35.

Cook, K. H., 1999: Generation of the African easterly jet and its role in determining West African precipitation. *J. Climate,* **12,** 1165–1184.

Folland, C. K., T. N. Palmer, and D. E. Parker, 1986: Sahel rainfall and worldwide sea temperatures, 1901–85. *Nature,* **320,** 602–607.

——, J. Owen, M. N. Ward, and A. Colman, 1991: Prediction of seasonal rainfall in the Sahel region using empirical and dynamical methods. *J. Forecasting,* **10,** 21–56.

Fontaine, B., S. Janicot, and V. Moron, 1995: Rainfall anomaly patterns and wind field signals over West Africa in August (1958–1989). *J. Climate,* **8,** 1503–1510.

Hastenrath, S., 1990: Decadal-scale changes of the circulation in the tropical Atlantic sector associated with Sahel drought *Int. J. Climatol.,* **10,** 459–472.

——, 1991: *Climate Dynamics of the Tropics.* Kluwer Academic, 488 pp.

Huffman, J., and Coauthors, 1997: The Global Precipitation Climatology Project (GPCP) Combined Precipitation Dataset. *Bull. Amer. Meteor. Soc.,* **78,** 5–20.

Hulme, M., 1994: Validation of large-scale precipitation fields in general circulation models. *Global Precipitation and Climate Change,* M. Debois and F. Desalmand, Eds., NATO ASI Series, Vol. 126, Springer-Verlag, 387–405.

Janicot, S., V. Moron, and B. Fontaine, 1996: Sahel droughts and ENSO dynamics. *Geophys. Res. Lett.,* **23,** 515–518.

——, S. Trzaska, and I. Poccard, 2001: Summer Sahel–ENSO teleconnection and decadal time scale SST variations. *Climate Dyn.,* **18,** 303–320.

Kershaw, R., and D. Gregory, 1997: Parametrization of momentum transport by convection. I: Theory and cloud modelling results. *Quart. J. Roy. Meteor. Soc.,* **123,** 1133–1151.

Kistler, R., and Coauthors, 2001: The NCEP–NCAR 50-year reanalysis: Monthly means CD-ROM and documentation. *Bull. Amer. Meteor. Soc.,* **82,** 247–268.

Lamb, P. J., 1978: Large-scale tropical Atlantic surface circulation patterns associated with sub-Saharan weather anomalies. *Tellus,* **30,** 240–251.

Lean, J., J. Beer, and R. Bradley, 1995: Reconstruction of solar irradiances since 1610: Implications for climate change. *Geophys. Res. Lett.,* **22,** 3195–3198.

Le Barbé, L., T. Lebel, and D. Tasoba, 2002: Rainfall in West Africa during the years 1950–90. *J. Climate,* **15,** 187–202.

Newell, R. E., and J. W. Kidson, 1984: African mean wind changes between Sahelian wet and dry periods. *J. Climatol.,* **4,** 27–33.

Nicholson, S. E., B. Some, and B. Kone, 2000: An analysis of recent rainfall conditions in West Africa, including the rainy seasons of the 1997 El Niño and the 1998 La Niña years. *J. Climate,* **13,** 2628–2640.

Palmer, T. N., 1986: Influence of Atlantic, Pacific and Indian Oceans on Sahel rainfall. *Nature,* **322,** 251–253.

Pope, V. D., M. Gallani, P. R. Rowntree, and R. A. Stratton, 2000: The impact of new physical parametrizations in the Hadley Centre climate model—HadAM3. *Climate Dyn.,* **16,** 123–146.

Rayner, N. A., D. E. Parker, E. B. Horton, C. K. Folland, L. V. Alexander, D. P. Rowell, E. C. Kent, and A. Kaplan, 2003: Global analyses of SST, sea ice and night marine air temperature since the late nineteenth century. *J. Geophys. Res.,* in press.

Rowell, D. P., 1990: Simulation of the tropical diurnal cycle in a climate model. Climate Research Tech. Note 3, Hadley Centre, Met Office, United Kingdom, 22 pp.

——, 2001: Teleconnections between the tropical Pacific and the Sahel. *Quart. J. Roy. Meteor. Soc.,* **127,** 1683–1706.

——, C. K. Folland, K. Maskell, J. A. Owen, and M. N. Ward, 1992: Modelling the influence of global sea surface temperatures on the variability and predictability of seasonal Sahel rainfall. *Geophys. Res. Lett,* **19,** 905–908.

——, C. K. Folland, K. Maskell, and M. N. Ward, 1995: Variability of summer rainfall over tropical North Africa (1906–92): Observations and modelling. *Quart. J. Roy. Meteor. Soc.,* **121,** 669–704.

Sato, M., J. E. Hansen, M. P. McCormick, and J. B. Pollack, 1993: Stratospheric aerosol optical depths, 1850–1990. *J. Geophys. Res.,* **98,** 22 987–22 994.

Shinoda, M., and R. Kawamura, 1994: Tropical rainbelt, circulation, and sea surface temperatures associated with the Sahelian rainfall trend. *J. Meteor. Soc. Japan,* **72,** 341–357.

Susskind, J., P. Piraino, L. Rokke, L. Iredell, and A. Mehta, 1997: Characteristics of the TOVS Pathfinder Path A dataset. *Bull. Amer. Meteor. Soc.,* **78,** 1449–1472.

Taylor, K. E., D. Williamson, and F. Zwiers, 2000: The sea surface temperature and sea-ice concentration boundary conditions for AMIP II simulations. PCMDI Rep. 60, Lawrence Livermore National Laboratory, Livermore, CA, 25 pp.

Thorncroft, C. D., and D. P. Rowell, 1998: Interannual variability of African wave activity in a GCM. *Int. J. Climatol.,* **18,** 1305–1323.

Trenberth, K. E., and C. J. Guillemot, 1998: Evaluation of the atmospheric moisture and hydrological cycle in the NCEP/NCAR reanalyses. *Climate Dyn.,* **14,** 213–231.

Vizy, E. K., and K. H. Cook, 2001: Mechanisms by which Gulf of Guinea and eastern North Atlantic sea surface temperature anomalies can influence African rainfall. *J. Climate,* **14,** 795–821.

von Storch, H., and F. W. Zwiers, 1999: *Statistical Analysis in Climate Research.* Cambridge University Press, 484 pp.

Ward, M. N., 1994: Tropical North-African rainfall and worldwide monthly to multi-decadal climate variations. Ph.D. thesis, University of Reading, 313 pp.

——, C. K. Folland, K. Maskell, A. Colman, D. P. Rowell, and K. Lane, 1993: Experimental seasonal forecasting of tropical rainfall at the U.K. Meteorological Office. *Prediction of Interannual Climate Variations,* J. Shukla, Ed., NATO ASI Series, Vol. 16, Springer-Verlag, 197–216.